SCIENCE CHINA
Chemistry

• MINI REVIEWS •
• SPECIAL TOPIC • Advances in Organic Optoelectronic Molecules & Materials

June 2015 Vol.58 No.6: 922–936
doi: 10.1007/s11426-015-5418-6

# Development of small-molecule materials for high-performance organic solar cells

Haijun Fan & Xiaozhang Zhu*

*Beijing National Laboratory for Molecular Sciences; CAS Key Laboratory of Organic Solids; Institute of Chemistry, Chinese Academy of Sciences, Beijing 100190, China*

Received January 1, 2015; accepted January 23, 2015; published online April 22, 2015

With the rapid development in recent years, small-molecule organic solar cell is challenging the dominance of its counterpart, polymer solar cell. The top power conversion efficiencies of both single and tandem solar cells based on small molecules have surpassed 9%. In this mini review, achievements of small molecules with impressive photovoltaic performance especially reported in the last two years were highlighted. The relationship between molecular structure and device performance was analyzed, which draws some rules for rational molecular design. Five series of p- and n-type small molecules were selected based on the consideration of their competitiveness of power conversion efficiencies.

**small-molecule solar cells, small-molecule donors, small-molecule non-fullerene acceptors, power conversion efficiency**

## 1 Introduction

As a promising technology developed for renewable energy sources by converting solar energy into electricity, organic solar cells have several potential advantages over the conventional inorganic solar cells, such as low overall cost, flexibility, and environmental friendliness [1]. Based on the natural difference of the donor materials used in organic photovoltaic (OPV) devices, they are briefly divided into polymer [2,3] and small-molecule solar cells [4]. Encouraging power conversion efficiencies (PCEs) for them have already been achieved, ~10.8% [5] and ~9.9% [6] respectively. From the aspect of PCE, small-molecule solar cells were developed even faster, which took only two years to accomplish the leap from 6.7% [7] to 9.9% [6]. The intensive researches on small-molecule solar cells have led to hundreds of scientific papers and several review articles were organized with certain viewpoints. In this mini review, we do not intend to repeat thorough statistic work, but select approximately 56 papers with competitive PCEs of over 5% for small-molecule donors, and over 3% for small-molecule acceptors that were reported in the last three years and make a systematic and sensible analysis to guide molecular design.

Compared with polymer counterparts, small molecules have well-defined molecular structure with definite molecular weight, giving several advantages of high purity, tunable electronic structures, and better device reproducibility. They can be mainly classified into two types: p-type small molecules and n-type small molecules, according to their functions as electron donors or electron acceptors in OPV devices. After surveying small-molecule solar cells with promising PCEs, we found it appropriate to catalogue them into five groups based on structural or functional features, benzothiadiazole-dicyanovinylene (BT-DCV)-capped molecules, thiophene-diketopyrrolopyrrole-thiophene (T-DPP-T)-containing molecules, squaraine derivatives, oligothiophene-based small-molecule donors, and PDI-based n-type small-molecule acceptors as shown in Figure 1.

*Corresponding author (email: xzzhu@iccas.ac.cn)

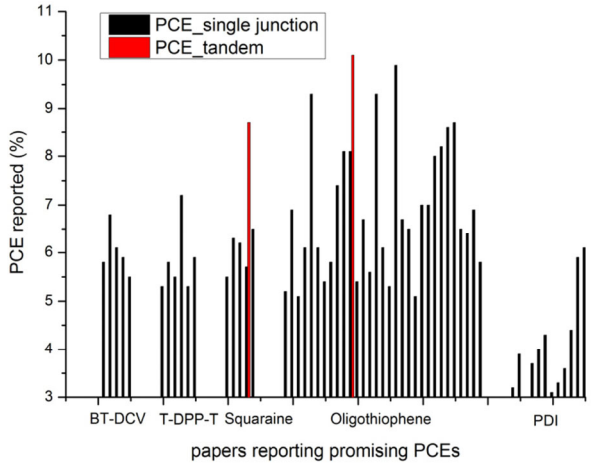


**Figure 1** Small-molecules series with promising PCEs.

## 2 BT-DCV-capped small molecules

BT-DCV-capped series are shown in Figure 2 with key parameters summarized in Table 1. In 2011, Lin *et al.* [8] uti-lized Compound **1** as a donor material for vacuum-deposited planar mixed heterojunction (PMHJ) solar cells, displaying a record PCE of 5.81%. Compound **1** has a D-A-A structure including two electron-withdrawing moieties, benzothiadiazole (BT) and dicyanovinylene (DCV), and one electron-donating moiety, ditolylaminothiophene. This strategy enables **1** to exhibit distinguished light-harvesting abilities with spectral responses close to the near-IR region, 1.55–1.77 eV, while maintains a relatively low-lying HOMO energy level, –5.30 eV, which contributed to high $V_{oc}$ of 0.79 V, and $J_{sc}$ of 14.68 mA/cm [2], in PMHJ solar cells incorporating C70 as the acceptor. Later in 2012, they continued this strategy and designed another molecule **2** with a benzene bridge that showed a PCE of up to 6.8% under optimized device conditions [9]. The trade-off between the photovoltage and photocurrent was achieved via delicate molecular engineering together with device optimization including fine tuning of the active-layer thickness and blend ratios of donor and acceptor materials.

The success of this small molecule series inspired further researches. In 2013, Lin *et al.* [10] discussed the effect of electron-transporting layer (ETL) in OPV devices based on this **1**:fullerene blend. Several pyridine-based electron transporting materials, TmPyPB, BCP, B3PyPB and DPPS, were compared in device performance. Among them, TmPyPB was proved to be the most effective ETL material since it rendered PCEs of up to 6.3%, showing ca. 10% enhancement compared with 2,9-dimethyl-4,7-diphenyl-1,10-phenanthroline (BCP). In 2014, they further reported solution

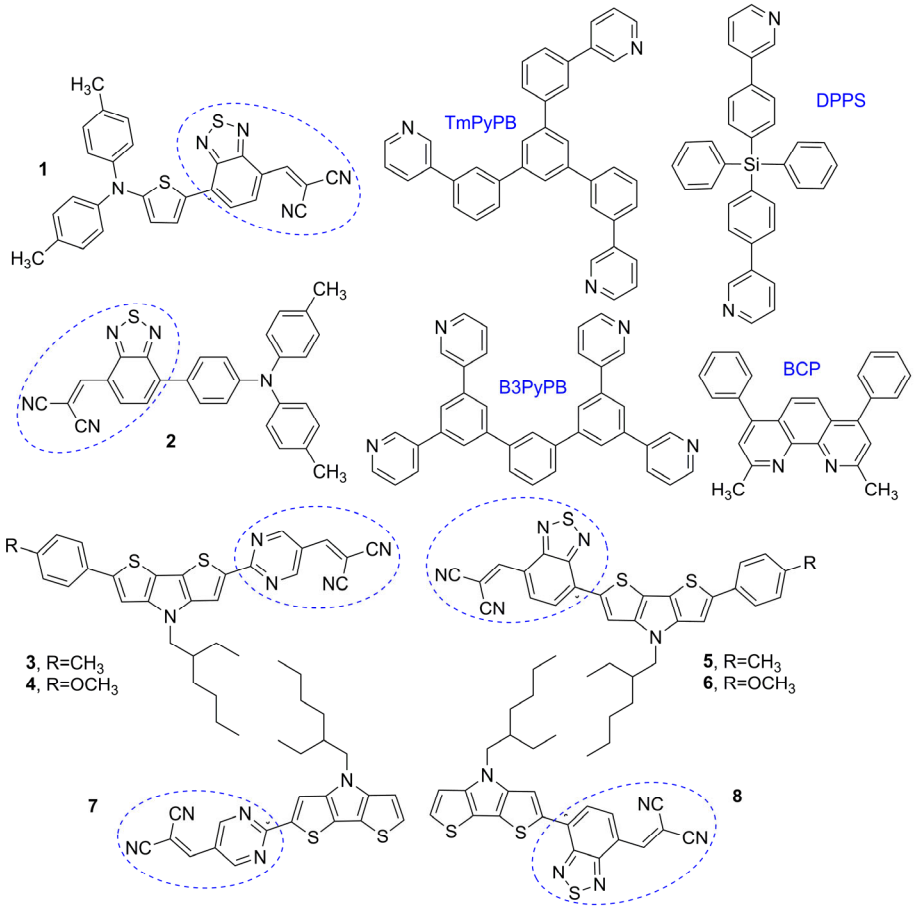


**Figure 2** BT-DCV-capped molecules and pyridine-based ETL materials.

processed OPVs using **2** and pristine C70, delivering a PCE of 5.9%, ~90% of those from devices by vacuum deposition [11]. This strategy is believed to be of generality for other organic D-A-A donors without long alkyl substitutions.

Besides, Wong *et al*. [12] performed extended researches based on this BT-DCV end-capped system. Pyrimidine was introduced to serve as a central electron-deficient unit. To further refine the D-A-A structure by modifying the donor moiety, the bulky terminal aryl groups attached to the tetrahedral N center, they replaced triarylamino groups with a rigid and planar dithienopyrrole (DTP) moiety in order to induce a sufficient electron coupling with the A-A component meanwhile reduce the conformational variations on the N center for getting better intermolecular interaction. Six molecules, **3**, **4**, **5**, **6**, **7**, and **8**, with D-A-A structures bearing DTP or aryl-substituted DTP as the D unit and BT-DCV or pyrimidine-DCV as the A-A block were synthesized. The systematic molecular structure-device performance analysis indicated that Compound **3** composed of a *p*-tolyl terminal group and DTP-pyrimidine-DCV, delivered the highest PCE of 5.6% with pristine C70 [12].

## 3 T-DPP-T-containing small molecules

Diketopyrrolopyrrole (DPP) as an attractive electron-withdrawing moiety has been utilized to construct photovoltaic materials in terms of facile synthetic modification and substitution of various aromatic groups on the 2,5-positions [13]. However, most DPP-based small-molecule materials only gave moderate PCEs of less than 5% [14,15]. Molecules with relatively high photovoltaic performance are summarized in Table 2, whose structures are shown in Figure 3. Noticing that all DPP units in these molecules are flanked with two thiophene (T) units, we thus ascribe this series as "T-DPP-T" containing small molecules.

In 2013, the first DPP-based small molecule, **9**, with PCEs of up to 5%, incorporating an alkylthiophene substituted benzodithiophene (BDTT) unit, was synthesized and reported by Yao *et al*. [16] and Zhan *et al*. [17], independently. Applying different acceptor materials, PC61BM or PC71BM, and different optimization procedures for photovoltaic devices, they obtained PCEs of 5.79% and 5.29% respectively. They demonstrated BDT unit was a promising building block for small-molecule donors. Marks *et al*. [18] reported another series of DPP-based molecular donor, **10**, with benzo[1,2-*b*:6,5-*b*′]dithiophene (*b*BDT) instead (Figure 3). Through fine tuning of aliphatic side chains and the processing additives, the self-organization properties of **10** in BHJ blends was improved. Molecule **10b** delivered a maximum PCE of 5.5%, which is comparable to those reported by Yao *et al.* [16] and Zhan *et al*. [17].

In the same year, Peng *et al*. [19] reported DPP-based small-molecule donor, **11**, and gained even higher PCEs. In their design, the porphyrin core was attached two T-DPP-T units by two triple carbon-carbon bonds. Modification of the substituents attached to porphyrin unit was made based on the consideration of increasing the intermolecular π-π stacking of the porphyrin core by using shorter alkyl chain. Photovoltaic devices optimized with 1,8-diiodo-octane

**Table 1** Photovoltaic parameters of organic solar cells based on BT-DCV-capped small molecules with PCEs of over 5%

| Device structure | Method | $V_{oc}$ (V) | $J_{SC}$ (mA/cm$^2$) | *FF* | $\eta$ [a] (%) | Ref. |
|---|---|---|---|---|---|---|
| ITO/$MoO_3$ (5 nm)/**1** (7 nm)/**1**:C70 (1:1 by volume, 40 nm)/C70 (7 nm)/BCP (10 nm)/Ag (150 nm) | PHJ, vac [b] | 0.79 | 14.68 | 0.50 | 5.8 | [8] |
| ITO/$MoO_3$ (5 nm)/**2** (7 nm)/**2**:C70 (1:1.6, 40 nm)/C70 (7 nm)/BCP (10 nm)/Ag (150 nm) | PHJ, vac [b] | 0.93 | 13.48 | 0.53 | 6.8 | [9] |
| ITO/$MoO_3$ (5 nm)/**1** (7 nm)/**1**:C70 (1:1.6 by volume, 40 nm)/C70 (7 nm)/TmTyPB (10 nm)/Ag (150 nm) | PHJ, vac [b] | 0.79 | 14.61 | 0.52 | 6.1 | [10] |
| ITO/Ca (1 nm)/**2**:C70 (1:2 by volume)/**2** (7 nm)/$MoO_3$ (7 nm)/Ag (120 nm) | BHJ, sol [c] | 0.95 | 13.4 | 0.46 | 5.9 | [11] |
| ITO/PEDOT:PSS (30 nm)/$MoO_3$ (5 nm)/**3** (7 nm)/**3**:C70 (1:2 by volume, 40 nm)/C70 (7 nm)/Bphen (6nm)/Ca (1 nm)/Ag | PHJ, vac [b] | 0.94 | 11.39 | 0.50 | 5.5 | [12] |

a) Measured under AM1.5G simulated solar illumination, 100 mW/cm$^2$, below the same except else indicated; b) vacuum deposition; c) solution fabrication.

**Table 2** Photovoltaic parameters of small-molecule solar cells based on T-DPP-T-containing small molecules with PCEs of over 5%

| Device structure | Method | $V_{oc}$ (V) | $J_{SC}$ (mA/cm$^2$) | *FF* | $\eta$ (%) | Ref. |
|---|---|---|---|---|---|---|
| ITO/PEDOT:PSS (30 nm)/**9**:PC71BM (1:1, 160–180 nm)/Ca (20 nm)/Al (80 nm) | BHJ, sol | 0.72 | 11.86 | 0.62 | 5.3 | [16] |
| ITO/PEDOT:PSS (30 nm)/**9**:PC61BM (1:1, 100 nm)/Ca (15 nm)/Al (50 nm) | BHJ, sol | 0.84 | 11.97 | 0.57 | 5.8 | [17] |
| ITO/ZnO (20 nm)/**10**:PC71BM (1:1, 1 vol% DIO)/$MoO_x$ (7.5 nm)/Ag (120 nm) | BHJ, sol | 0.77 | 11.4 | 0.63 | 5.5 | [18] |
| ITO/PEDOT:PSS (40 nm)/**11**:PC61BM (1:1.2, *w*/*w*, .4 vol% DIO, 140 nm)/PFN (0.02 *w*/*v* in methanol)/Al (80 nm) | BHJ, sol | 0.71 | 16.0 | 0.64 | 7.2 | [19] |
| ITO/PEDOT:PSS (40 nm)/**12**:PC71BM/Ca (20 nm)Al (120 nm) | BHJ, sol | 0.63 | 14.6 | 0.58 | 5.3 | [20] |
| ITO/PEDOT:PSS/**14**:PC61BM (1:2, *w*/*w*)/Au (100 nm) | BHJ, sol | 0.93 | 14.86 | 0.43 | 5.9 | [21] |

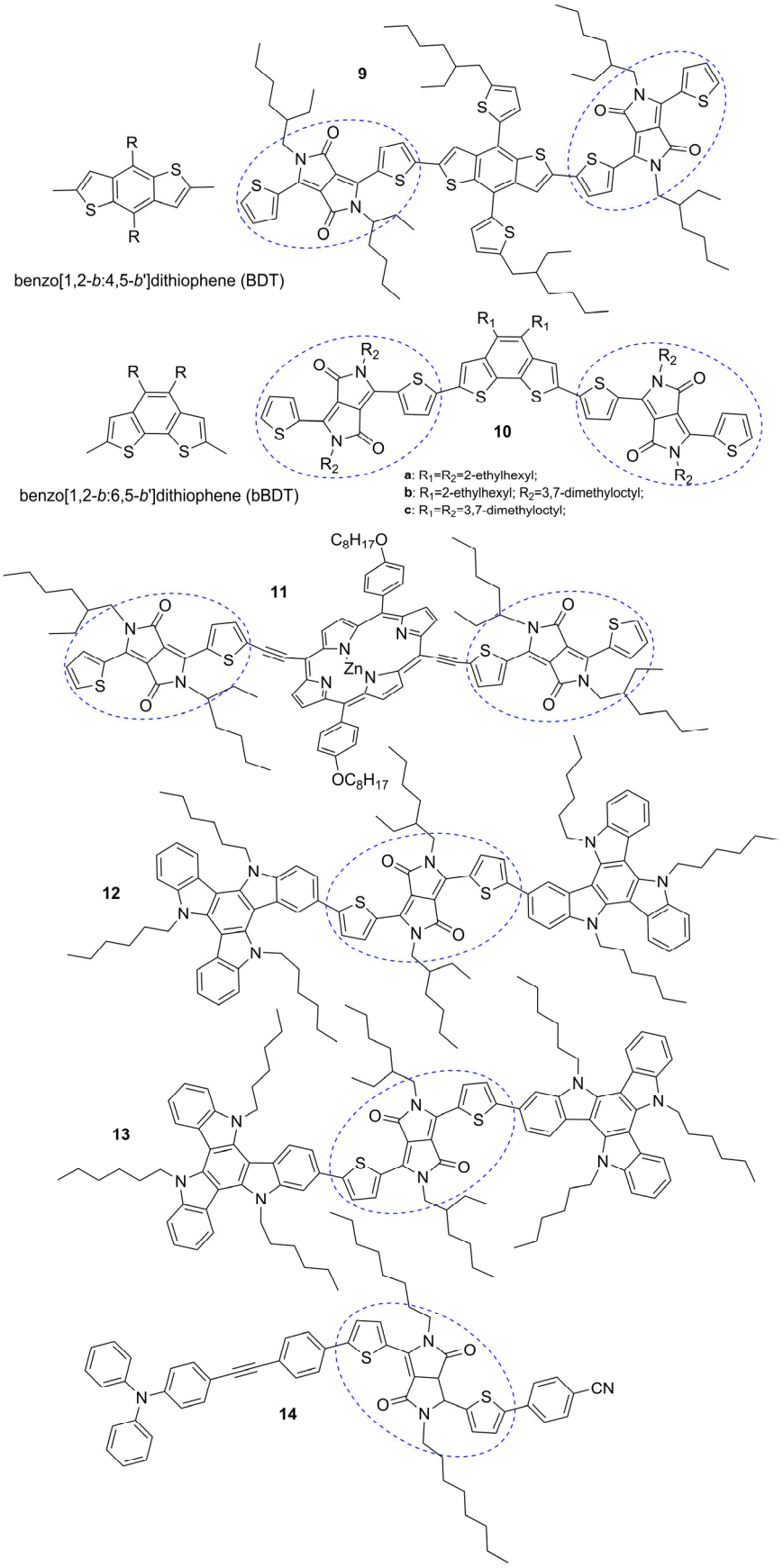


**Figure 3** T-DPP-T-containing small molecules.

(DIO) additive based on **11** and PC61BM showed significantly enhanced PCEs, reaching a record of 7.23% among all reported PCEs in this series.

Molecular donors with only one T-DPP-T block also showed comparable results. Ziessel *et al*. [20] reported a dumbbell-shaped triazatruxene (TAT)-diketopyrrolopyrrole (DPP)-triazatruxene (TAT) molecule in 2013, with two regioisomers **12** and **13** (Figure 3). The *para*-isomer, **12**, gave higher PCEs of up to 5.3% because it promoted end-to-end π-π interactions in solid state and leads to favorable active-layer morphology when blended with PC71BM. Later Yin *et al*. [21] reported an unsymmetrical push-pull small molecule, **14**, using triphenylamine (TPA) and DPP as the main building blocks, yielding a PCE of 5.94%.

## 4 Squaraine derivatives

Squaraine (SQ) was firstly introduced to OPV applications by Marks *et al*. [22] in 2008 since SQ molecules generally show broad absorption (from 500 to 900 nm in thin films), high absorption coefficients of exceeding $10^5$ L/(mol cm), and good photochemical and thermal stability. Intensive researches have been made, yet inspiring results are still few. The countable SQ donors of PCEs over 5% are contributed by Forrest *et al*. [23–28] as shown in Figure 4, corresponding device structures and photovoltaic parameters being summarized in Table 3.

Among the four molecules, the OPV application of Compound **15** was firstly reported in 2011. By solvent annealing under dichloromethane atmosphere, **15**:PC71BM blends gained optimized morphology that reduced the specific series resistance ($R_{SA}$), and hence increased the fill factor (*FF*), yielding a maximum PCE of 5.5% ($V_{oc}$=0.92 V, $J_{sc}$=12.0 mA/cm$^2$, *FF*=0.50) [23]. Later on, they developed another SQ-based molecular donor, **16**, by substitution of isobutylamino group with bulky arylamino groups. The weaker electron-donating arylamino groups resulted in a deeper HOMO energy level. Devices based on 16/C60 showed larger $V_{oc}$, 0.91 V, and a maximum PCE of up to 6.3% after thermal annealing [24]. Interestingly, device performance of **16** can be further improved by using SQ donor blends. For example, when blending **16** with another asymmetric squaraine donor, **17**, with short absorption ($\lambda_{abs}^{max}$: 530 nm) [25], a maximum PCE of 6.2% can be achieved because donor mixture partially fills the valley in EQE spectra between 500 and 600 nm [26]. They also applied this donor1/donor2:acceptor blending method to other SQ-based solar cells. By careful control of the "inverted" quasi-epitaxial growth, the voltage loss in **17**:**18**/C70 devices was minimized, resulting in the best PCE of 5.7% in single junction devices among this series. Furthermore, tandem solar cells based on **17**:**18**/C70 and tetraphenyldibenzoperiflanthene (DBP):C70 systems were reported, delivering an impressive PCE of up to 8.7% [27]. Similarly, optimized tandem solar cells incorporating two solution-processed **17**:**18**/C70 active layers were also disclosed, yielding a PCE of 6.5% under AM1.5G, 70 mW/cm$^2$ [28].

## 5 Oligothiophene (OT)-based small molecules

OT-based small molecules are mostly well developed among all small-molecule donors, as evidenced by a large numbers of papers. We separated these molecules into 3 subclasses for an easy description, namely oligothiophenes, BDT-T-based, and DTS-BT-T-based small molecules, which are shown in Figures 5–7. The photovoltaic parameters for their optimized devices are summarized in Table 4.

Bäuerle *et al*. [29] synthesized a series of DCV substituted oligothiophenes and studied the relationship between chain length and photovoltaic performance in 2011, obtaining a PCE of 5.2% for vacuum-deposited BHJ devices with Compound **19** and C60. Later they reported **20** after systematically varying the methyl substitution pattern along the conjugated backbone, showing a PCE of 6.1% by **20**:C60 vacuum-deposited BHJ device. Further optimization of the processing parameters during device fabrication using **20** afforded a highest PCE of 6.9% by reducing electrode absorption and increasing back-contact reflectance [30]. Chen *et al*. [31] reported **21** with octylcyanoacetate end group, delivering a PCE of 5.08% for solution processed **21**:PC61BM devices. They made further modifications on this molecule to enhance the sunlight absorption meantime

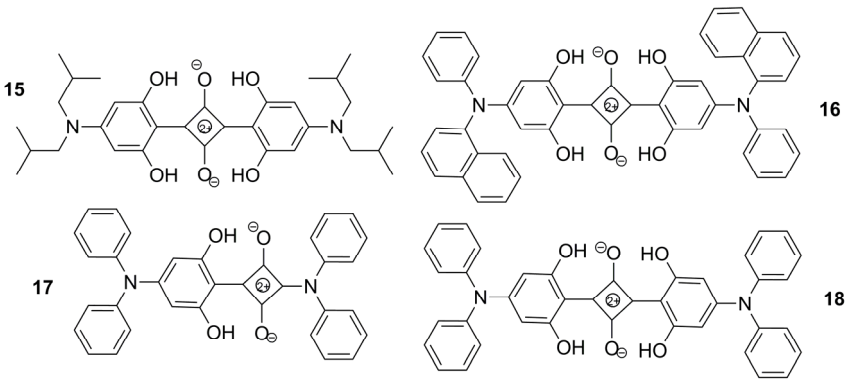


**Figure 4** Squaraine derivatives.

**Table 3** Photovoltaic parameters of squaraine-based small molecule solar cells with PCEs of over 5%

| Device structure | Method | $V_{oc}$ (V) | $J_{SC}$ (mA/cm$^2$) | *FF* | $\eta$ (%) | Ref. |
|---|---|---|---|---|---|---|
| ITO/$MoO_3$ (8 nm)/**15**:PC71BM (1:6,78 nm)/C60 (4 nm)/BCP (1 nm)/LiF (0.8 nm)/Al (100 nm) | BHJ, sol | 0.92 | 12.0 | 0.50 | 5.5 | [23] |
| ITO/$MoO_3$ (8 nm)/**16** (20 nm)/C60 (40 nm)/BCP (10 nm)/Ag (100 nm) | BHJ, sol | 0.91 | 11.1 | 0.65 | 6.3 | [24, 25] |
| ITO/$MoO_3$ (8nm)/**16**:**17** (0.5:1, *w*/*w*, 20 nm)/C60 (40 nm)/PTCBI (8 nm)/Ag (100 nm) | PHJ, vac | 0.80 | 11.0 | 0.73 | 6.2 | [26] |
| ITO/$MoO_3$ (15 nm)/**17**:**18** (4:6, *w*/*w*, 16 nm)/C70 (10 nm)/PTCBI (8 nm)/Ag (100 nm) | PHJ, vac | 0.93 | 9.8 | 0.65 | 5.7 | [27] |
| ITO/$MoO_3$ (20 nm)/**17**:**18** (4:6, *w*/*w*, 16 nm)/C70 (10 nm)/PTCBI (5 nm)/Ag (0.1 nm)/$MoO_3$ (5 nm)/DBP:C70 (25 nm)/C70 (7 nm)/BPhen (7 nm)/Ag (100 nm) | Tandem, vac | 1.86 | 7.8 | 0.62 | 8.7 | |
| ITO/$MoO_3$ (20 nm)/**17**:**18** (4:6, *w*/*w*, 16 nm)/C70 (10 nm)/PTCBI (5 nm)/Ag (0.1 nm)/$MoO_3$ (7 nm)/**17**:**18** (4:6, *w*/*w*, 15 nm)/C60 (28 nm)/PTCBI (5 nm)/100 nm Ag | Tandem, vac | 1.79 | 5.22 | 0.68 | 6.5 [a] | [28] |

a) Measured under AM1.5G simulated solar illumination, 70 mW/cm$^2$.

**Table 4** Photovoltaic parameters of oligothiophene-based small molecule solar cells with PCEs of over 5%

| Device structure | Method | $V_{oc}$ (V) | $J_{sc}$ (mA/cm$^2$) | *FF* | $\eta$ (%) | Ref. |
|---|---|---|---|---|---|---|
| ITO/C60:NDN1 (2% doped, 5 nm)/**19**:C60 (40 nm)/BPAPF (5 nm)/BPAPF:NDP9 (10% doped, 10 nm)/Spiro-NPD:NDP9 (10%, 30 nm)/Al (50 nm) | BHJ, vac | 0.97 | 11.1 | 0.49 | 5.2 | [29] |
| ITO/C60 (15 nm)/**20**:C60 (30 nm, 2:1 *v*/*v*, 90 °C substrate) **14**/BPAPF (5 nm)/BPAPF:NDP9 (50 nm, 90:10 *w*/*w*)/NDP9 (1 nm)/Au (50 nm) | BHJ, vac | 0.96 | 11.1 | 0.66 | 6.1 | [30] |
| ITO/C60:W2(hpp)4 (5 nm, 96:4 *w*/*w*)/C60 (15 nm)/**20**:C60 (30 nm, 2:1 *v*/*v*, 75 °C substrate)/BPAPF (5 nm)/BPAPF:NDP9 (50 nm, 90:10 *w*/*w*)/NDP9 (2 nm)/Al (100 nm) | BHJ, vac | 0.95 | 11.5 | 0.63 | 6.9 | |
| ITO/PEDOT:PS (40 nm)/**21**:PC61BM (1:0.5, 120–150 nm)/Ca (20 nm)/Al (80 nm) | BHJ, sol | 0.86 | 10.7 | 0.55 | 5.1 | [31] |
| ITO/PEDOT:PSS (40 nm)/**22**:PC61BM (1:0.5, 65–110 nm)/LiF (0.8 nm)/Al (60 nm) | BHJ, sol | 0.92 | 14.0 | 0.47 | 6.1 | [32] |
| ITO/PEDOT:PSS/**23**:PC71BM (1:0.5, 120 nm)/PFN (5 nm)/Al (80 nm) | BHJ, sol | 0.91 | 14.87 | 0.69 | 9.30 | [6b] |
| TO/PEDOT:PSS (40 nm)/**24**:PC71BM (1:1.2, 0.1 mg/mL PDMS, 120–130 nm)/Ca (20 nm)/Al (100 nm) | BHJ, sol | 0.85 | 10.79 | 0.67 | 6.1 | [33] |
| ITO/PEDOT:PSS (40 nm)/**25**:PC61BM (1:0.5, 110 nm)/LiF (0.8 nm)/Al (60 nm) | BHJ, sol | 0.93 | 9.77 | 0.60 | 5.4 | [34] |
| ITO/PEDOT:PSS (40 nm)/**26**:PC61BM (1:0.8, 130 nm)/LiF (0.8 nm)/Al (60 nm) | BHJ, sol | 0.80 | 11.5 | 0.64 | 5.8 | [35] |
| ITO/PEDOT:PSS (40 nm)/**27**:PC71BM (1:0.8, 100 nm)/LiF (0.8 nm)/Al (80 nm) | BHJ, sol | 0.93 | 12.2 | 0.65 | 7.4 | [36] |
| ITO/PEDOT:PSS (40 nm)/**28**:PC71BM (1:0.8)/LiF (0.8 nm)/Al (80 nm) | BHJ, sol | 0.93 | 13.2 | 0.66 | 8.1 | [37] |
| ITO/PEDOT:PSS (40 nm)/**29**:PC71BM (1:0.8, 120 nm)/Ca (20 nm)/Al (100 nm) | BHJ, sol | 0.94 | 12.5 | 0.69 | 8.1 | [38] |
| ITO/PEDOT:PSS (40 nm)/**29**:PC71BM (1:0.8, 80 nm)/CPE1 (0.02 wt%, 5 nm)/CPE2 (0.02 wt%, 5 nm)/M-PEDOT:PSS/29:PC71BM (1:0.8, 100 nm)/CPE3 (0.02 wt%)/Al (100 nm) | Tandem, sol | 1.82 | 7.70 | 0.72 | 10.1 | |
| ITO/PEDOT:PSS (30 nm)/**30**:PC61BM (1:0.4)/Ca (30 nm)/Al (100 nm) | BHJ, sol | 0.90 | 9.08 | 0.66 | 5.4 | [39] |
| ITO/PEDOT:PSS (30 nm)/**31**:PC71BM (1.5:1)/Ca (30 nm)/Al (70 nm) | BHJ, sol | 0.92 | 11.0 | 0.66 | 6.7 | [40] |
| ITO/PEDOT:PSS (30 nm)/**32**:PC71BM (1:1.2)/Ca (20 nm)/Al (100 nm) | BHJ, sol | 0.87 | 9.94 | 0.65 | 5.6 | [41] |
| ITO/PEDOT:PSS/**33**:PC71BM (1:1, 250 nm)/Ca (40 nm)/Al (100 nm) | BHJ, sol | 0.90 | 13.90 | 0.74 | 9.3 | [6c] |
| ITO/PEDOT:PSS (10 nm)/**34**:PC61BM (1:2, 90–98 nm)/LiF (0.3 nm)/Al (120 nm) | BHJ, sol | 0.84 | 10.1 | 0.72 | 6.1 | [42] |
| ITO/PEDOT:PSS (35 nm)/**35**:PC71BM (1:3)/Ca (20 nm)/Al (100 nm) | BHJ, sol | 0.90 | 11.5 | 0.49 | 5.3 | [43] |
| ITO/PEDOT:PSS/**36**:PC71BM (1:0.8)/ETL-1/Al (80 nm) | BHJ, sol | 0.92 | 14.63 | 0.74 | 9.9 | [6a] |
| ITO/$MoO_x$ (9 nm)/**37**:PC71BM (7:3, 180 nm)/Al (100 nm) | BHJ, sol | 0.78 | 14.4 | 59.3 | 6.7 | [7] |
| ITO/$MoO_x$ (9 nm)/**38**:PC71BM (7:3)/Al | BHJ, sol | 0.77 | 14.0 | 0.60 | 6.5 | [44] |
| ITO/$O_2$-NiO/**39**:PC61BM (7:3)/Ca (20 nm)/Al (100 nm) | BHJ, sol | 0.73 | 12.3 | 0.56 | 5.1 | [45] |
| ITO/PEDOT:PSS/**39**:PC71BM (3:2, 100 nm)/Ca (5 nm)/Al (100 nm) | BHJ, sol | 0.81 | 12.8 | 0.68 | 7.0 | [46] |
| ITO/PEDOT:PSS/**39**:PC71BM (3:2, 90–110 nm)/Ca (10 nm)/Al (100 nm) | BHJ, sol | 0.81 | 12.8 | 0.68 | 7.0 | [47] |
| ITO/PEDOT:PSS (30 nm)/**39**:PC71BM (3:2, 100 nm)/Ca (20 nm)/Al (80 nm) | BHJ, sol | 0.77 | 14.2 | 0.73 | 8.0 | [48] |
| ITO (5 Ω/□)/PEDOT:PSS (35 nm)/**39**:PC71BM (3:2, 0.4 vol% DIO, 100 nm)/Ca (20 nm)/Al (100 nm) | BHJ, sol | 0.77 | 14.74 | 0.72 | 8.2 | [49] |
| ITO/PEDOT:PSS (30 nm)/**39**:PC71BM (3:2)/Ba (20 nm)/Al (100 nm) | BHJ, sol | 0.77 | 14.96 | 0.74 | 8.6 | [50] |
| ITO/PEDOT:PSS (0.3 wt% Au NPs, 30 nm)/**39**:PC71BM (3:2, 1 wt% Au NRs), 100 nm/Ca (20 nm)/Ag (100 nm) | BHJ, sol | 0.77 | 15.56 | 0.71 | 8.7 | [51] |
| ITO/$MoO_x$ (9 nm)/**40**:PC71BM (1:1)/Al (100 nm) | BHJ, sol | 0.71 | 14.2 | 0.65 | 6.5 | [52] |
| ITO/PEDOT:PSS/**41**:PC71BM (1:1, 100 nm)/Ca (15 nm)/Al (100 nm) | BHJ, sol | 0.91 | 11.0 | 0.65 | 6.4 | [53] |
| ITO/PEDOT:PSS/**42**:PC71BM (3:2, 0.4% *v*/*v* DIO, 100 nm)/Ca (10 nm)/Al (100 nm) | BHJ, sol | 0.75 | 13.1 | 0.70 | 6.9 | [54] |
| ITO/ZnO/**42**:PC71BM (3:2, 0.4% *v*/*v* DIO, 100 nm)/$MoO_3$ (5 m) Ag (100 nm) | | 0.75 | 13.6 | 0.66 | 6.7 | |
| TO/PEDOT:PSS (50 nm)/**43**:PC71BM (1:2)/Al (90 nm) | BHJ, sol | 0.78 | 12.8 | 0.58 | 5.8 | [55] |

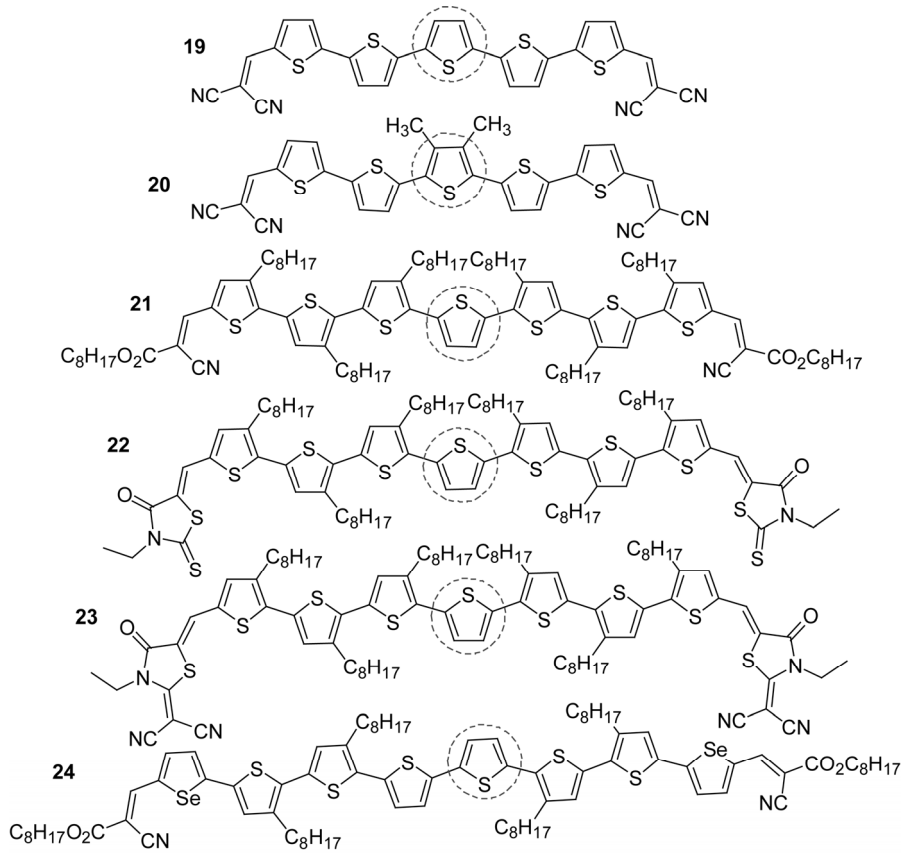


**Figure 5** The structure of oligothiophenes.

avoid changing molecular backbone and corresponding film morphology too much, by introducing 3-ethylrhodanine moiety. The new oligothiophene-based molecular donor, **22**, delivered a landmark PCE of 6.10% in **22**:PC61BM devices [32]. Further modification on molecule **22**, by replacing the sulfur atom on rhodanine end group with a malononitrile unit, has generated another effective molecular donor, **23**, which yields an even higher PCE of 9.30% [6b]. Yang *et al*. [33] also reported a modified oligothiophene with selenophene linkers, **24**, showing a comparable PCE of 6.15% to **22**.

Chen *et al*. modified the thiophene-only backbones of **19** and **22** by introducing BDT and dithienosilole (DTS) unit respectively, both bearing fused and planar configuration of potential of increasing the mobility and solar absorption. Two molecules, **25** and **26** (Figure 6), yielded high PCEs of 5.44% [34] and 5.84% [35] respectively. These PCE improvements can be ascribed to the large and rigid planar conjugated structures which facilitate the electron delocalization, and enhanced the π-π stacking in the solid state. Further modification of Compound **25** by end group engineering or substituents on BDT units, two typical molecules with optimized structures, **27** and **28**, were obtained, leading to PCEs of 7.38% [36] and 8.12% [37] (certified 7.61%) respectively. Yang *et al*. [38] reported **29** of 8.02% efficiency for single junction BHJ solar cells and 10.1% for homo-tandem solar cells, with molecular structure slightly different to **28** that uses a 3-octylrhodanine end group instead of 3-ethyl-rhodanine. Other three groups also studied this BDTT framework by modifying the end groups or the side chains. Chu *et al.* [39] reported a molecule capped with octylcyanoacetate, **30**, giving a PCE of 5.42% with PC61BM. Li *et al*. [40] introduced an indenedione (ID) unit for BDTT backbone and optimized the number of thiophene unit, reporting a BDTT-ID donor **31** bridged by two thiophene units showing optimized PCEs of up to 6.75%. Wei *et al*. [41] reported that PCE improvement could be made by modulating the molecular stacking through systematically shortening the alkyl chains attaching to the backbone thiophene units and end groups. The optimized molecule **32** gave a PCE of 5.6% with PC71BM. Recently Sun *et al*. [6c] reported a BDTT-based molecular donor, **33**, which exhibited typical nematic liquid crystalline behavior and displayed excellent photovoltaic property. Devices made of this material can afford high *FF* (~70%) and PCE (~8%) even with ~400 nm thick active layer, reporting a maximum PCE of 9.3%. Meantime, other groups focusing on modifying the main structure of BDT also reported promising results. Wessendorf *et al*. [42] replaced BDT with dithienopyrrole (DTP) and synthesized a series of oligomers with different alky chains on the N atoms. Compound **34** gave 6.1% PCE under the optimized condition. Zhan *et al*. [43]

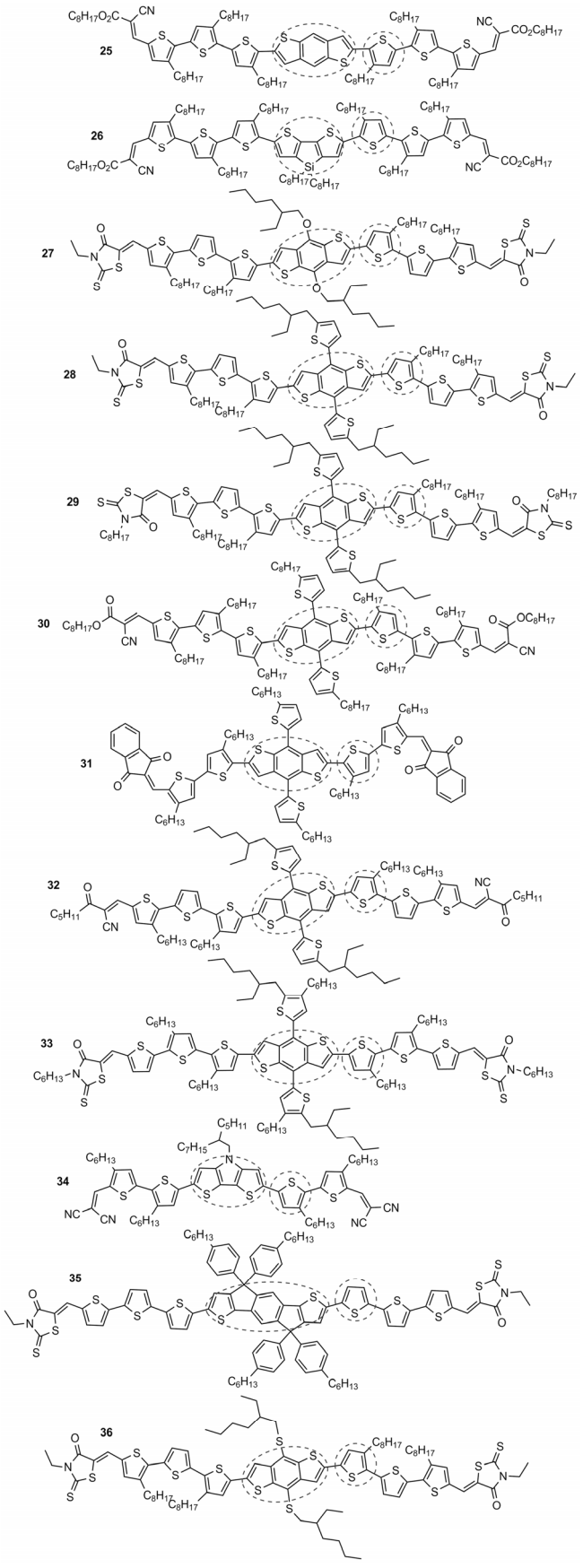

**Figure 6** BDT-T-based small molecules.

introduced another rigid and planar building block, indaceno[2,1-*b*:6,5-*b*′]dithiophene (IDT) and synthesized a series of molecules, in which molecule **35** gave a PCE of 5.32%. In 2014, Chen *et al*. [6a] disclosed a new modification on BDT unit, by replacing the oxygen atom in **27** to sulfur atom. The resultant molecule **36** released an inspiring PCE of 9.95% under optimized conditions via a combined thermal annealing-solvent vapor annealing method, which is the highest PCE reported up to now for single-junction SMOSCs.

Bazan and coworkers focused on DTS-BT-T-based small molecules that feature the same or similar backbones composing three kinds of building blocks, dithienosilole (DTS) unit, benzothiadiazole (BT) or pyridalthiadiazole (PT) unit, and thiophene (T) unit. In 2012, they reported a model DTS-PT-T molecule, **37** (Figure 7), and a record PCE of 6.7% [7]. Trace impurities from the synthesis can significantly influence the photovoltaic performance, causing a ~50% reduction in PCE [44]. Olson *et al.* [45] used its isomer **38** as the donor to blend with PC61BM, and systemically investigated the influence of hole-transport-layer and interfacial chemistry on device performance, reporting a maximum PCE of 5.1%. Bazan *et al*. further modified the molecular backbone by introducing a fluorobenzothiadiazole (FBT) unit to replace the PT unit. They obtained molecule **39** [46], with a PCE of 7.0% achieved by delicate morphology control [47]. Heeger *et al*. made systematic optimizations for this small molecule system with different methods yielding 8.01% [48], 8.24% [49] and 8.57% [50] PCEs, respectively. Sun *et al*. [51] also reported an enhancement of PCE up to 8.72% by simultaneously incorporating Au nanospheres into the hole transport layer and Au-silica nanorods into the active layer for this small molecule system. In 2014, Liu *et al*. [52] reported a series of molecules incorporating DTS, BT (PT or FBT), and T units. Most of these molecules displayed high PCEs of >5%, and the best one, **40**, gave a 6.5% value. Besides, Nguyen *et al*. [53] also disclosed a new high-efficiency molecular donor, **41**, incorporating a weak silaindacenodithiophene (SIDT) electron-donating fragment, showing a PCE of up to 6.4%. Sequentially, Sun *et al*. [54] replaced the DTS unit with a dithienogermole (DTG) following the strategy of replacing the central bridging carbon atom with a silicon atom or silicon with germanium in polymer design due to the consideration of increasing the intermolecular π-π interaction. However, the results showed different effect for this **42**:PC71BM small-molecule system, namely that the substitution of a silicon atom by a germanium atom in the small-molecule donor did not significantly change the thermal, electrical, and optical properties, nor the order of molecules increased. A comparable PCE of 6.9% to its Si-counterpart was reported. In the same year, Ko *et al*. [55] synthesized star shaped small molecules incorporating a triphenylamine (TPA) core and DTS-PTDZ- T arms, **43**, with efficiency also reaching 5.81%.

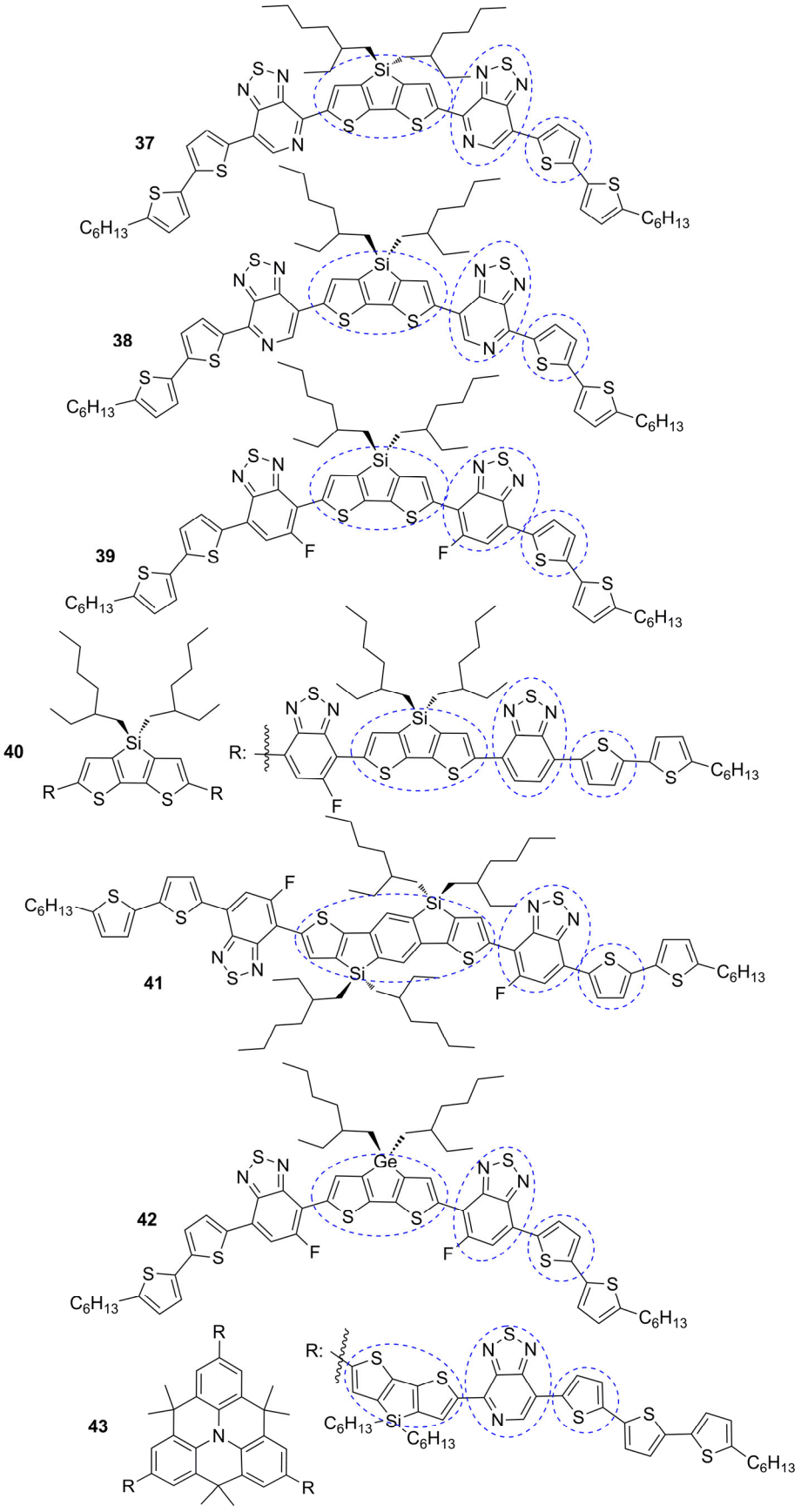


**Figure 7** DTS-BT-T-based small molecules.

## 6 PDI-based small molecule acceptors

Though fullerene derivatives are dominating as n-type materials for organic photovoltaic (OPV) application, incentive of developing non-fullerene acceptors [56] with comparable LUMO energy levels to fullerenes and extended spectrum response is becoming strong. Among all non-fullerene acceptors reported up to now [57], perylene diimides (PDIs) have attracted the most interest because of their excellent photo-stability, strong absorption in visible region, high electron mobility, and similar electron affinity to fullerenes. The tailoring of PDIs is convenient by varying substituents on nitrogen atoms or on the perylene core. Their applications in OPVs have been reported, leading to a maximum PCE of 6.05%. PDI acceptors with PCEs of over 3% have been collected (Table 5) and discussed as follow.

In 2010, Mikroyannidis *et al*. reported two PDI-based acceptors, **44** and **45** (Figure 8), displaying PCEs of 3.17% [58] and 3.88% [59] with two small molecule donors respectively. Two acceptors have different polycyclic aromatic hydrocarbons (PAHs) moieties attached to the N atoms. Bazan *et al*. [60] reported a PCE of 3.0% for a non-fullerene OPV, utilizing **39** as the donor and *N*,*N*′-bis(1-ethylpropyl)-perylene-3,4,9,10-tetracarboxylic diimide (**46**) bearing short branched alky chains on N atoms as the acceptor. Keivanidis *et al*. [61] also applied this acceptor but with a polymer, PBDTTT-CT, reporting a PCE of 3.7%. Other groups initialized molecular engineering aiming at weakening the strong aggregation of PDI derivatives [62], a drawback generally resulting in strong self-trapping of excitons. Yao *et al*. [63] reported a PDI-dimer-based acceptor, **47**, in which two PDI units were linked by a thiophene bridge. Significantly reduced aggregation was observed in PBDTTT-CT:**47** blend films, rendering a high PCE of 4.03%. Later they reported an enhanced PCE of up to 4.34% by a similar system, PBDTTT-CT:**48**, in which the PDI acceptor was modified by methoxyl chains instead of methoxyethoxyl chains [64]. Most recently, they reported an improved PCE of 6.1% for PBDTTT-CT:**47** devices through delicate control over the film-formation kinetics of the active layer [65]. Differently, Zhan *et al*. [66] introduced a bulky fused indacedithiophene (IDT) to bridge two PDI units and obtained **49** with a dihedral angle of ca. 49.6°, which delivered a PCE of up to 3.12%. Furthermore, they synthesized a star shaped PDI acceptor, **50**, in which triphenylamine core was used, reporting a PCE of 3.32% [67]. Yan *et al*. highlighted the importance of selecting matched donor materials for PDI acceptors and reported an highly matched PffBT4T-2DT:**51** blend system, yielding a 6.3% PCE [68], in which the PDI acceptor **51** also adopts a fused linkage unit, spirobifluorene [69]. Besides, they also reported a PDI acceptor of unique 3D molecular structure, **52**, with four PDIs linked together by a highly twisted tetraphenylethylene unit, which displayed a 5.53% PCE when blended with PBDTT-F-TT [70]. Hou *et al*. [71] reported a PDI dimer **53** in which PDI units were connected with a single bond at the bay position, achieving a PCE of 3.63% with PBDTTT-CT as the donor. Molecule **54** was obtained by fine-tuning the bay-linkages as well as the an improved PCE for this PDI acceptor by blending it with another polymer donor, PBDTBDD, which owns a down-shifted HOMO level and also shows strong aggregation effect in solution state that favors morphology tuning. Through careful device optimization they achieved a considerably high PCE of 4.39% [72]. Similarly, Jen *et al*. [73] reported an even higher PCE up to 5.9% by blending **53** with another polymer donor PBDTT-F-TT and combining molecular, interfacial, and device engineering. Quite recently, Nuckolls *et al*. [74] revealed that fused helical PDI **54** also yielded PCE up to 6.1% by PBDTT-TT:**54** devices. In virtue of femtosecond transient absorption spectroscopy, it was

**Table 5** Photovoltaic parameters of solar cells with PDI-based small molecule acceptors of PCEs over 5%

| Device structure | Method | $V_{oc}$ (V) | $J_{SC}$ (mA/cm$^2$) | *FF* | $\eta$ (%) | Ref. |
|---|---|---|---|---|---|---|
| ITO/PEDOT:PSS/T:**44** (1:3.5, 80–90 nm)/ZnO/Al | BHJ, sol | 0.95 | 6.3 | 0.53 | 3.2 | [58] |
| ITO/PEDOT:PSS/Se-SM:**45** (1:3.5, 100 nm)/Al | BHJ, sol | 0.90 | 8.30 | 0.52 | 3.9 | [59] |
| ITO/PEDOT:PSS (45 nm)/**39**:**46** (1:1, 0.4 vol% DIO)/Ca (5 nm)/Ag (100 nm) | BHJ, sol | 0.78 | 7.4 | 0.52 | 3.0 | [60] |
| ITO/ZnO/PBDTTT:**46** (3:7)/$V_2O_5$ (2 nm)/Ag (70 nm) | BHJ, sol | 0.81 | 8.16 | 0.53 | 3.7 | [61] |
| ITO/PEDOT:PSS (30 nm)/PBDTTT-C-T:**47** (1:1, 5 vol% DIO)/Ca (20 nm)/Al (80 nm) | BHJ, sol | 0.85 | 8.86 | 0.54 | 4.0 | [63] |
| ITO/PEDOT:PSS (30 nm)/PBDTTT-C-T:**48** (1:1, 2 vol% DIO, 90 nm)/$MnO_x$ (5 nm)/Ag (80 nm) | BHJ, sol | 0.79 | 10.17 | 0.55 | 4.3 | [64] |
| ITO/PEDOT:PSS (30 nm)/PBDTTT-C-T:**47** (1:1, 1.5 vol% DIO)/Ca (20 nm)/Al (80 nm) | BHJ, sol | 0.84 | 12.83 | 0.56 | 6.1 | [65] |
| ITO/PEDOT:PSS/9:**49** (1:1)/Ca (20 nm)/Al (50 nm) | BHJ, sol | 0.95 | 7.75 | 0.42 | 3.1 | [66] |
| ITO/PEDOT:PSS/PBDTTT-CT:**50**/(1:1, 5 vol% DIO, 100 nm)/Ca (15 nm)/Al (60 nm) | BHJ, sol | 0.88 | 11.92 | 0.34 | 3.3 | [67] |
| ITO/ZnO/PffBT4T-2DT:**51**/$V_2O_5$/Al | BHJ, sol | 0.99 | 11.1 | 0.58 | 6.3 | [68] |
| ITO/ZnO/PBDTT-F-TT:**52** (1:1.4, ~90 nm)/$V_2O_5$ (20 nm)/Al (100 nm) | BHJ, sol | 0.91 | 11.7 | 0.52 | 5.5 | [70] |
| ITO/PEDOT:PSS (35 nm)/PBDTTT-C-T:**53** (1:1, 1.5 vol% DIO+1.5 vol% CN)/Ca (20 nm)\|Al (80 nm) | BHJ, sol | 0.73 | 10.58 | 0.47 | 3.6 | [71] |
| ITO/PEDOT:PSS/PBDTBDD:**54** (1:1, 1.5 vol% DIO+1.5 vol% CN)/Ca (20 nm)/Al (80 nm) | BHJ, sol | 0.87 | 8.26 | 0.611 | 4.4 | [72] |
| ITO/ZnO (30 nm)/PBDTT-F-TT:**53**/$MoO_3$ (8 nm)/Ag (100 nm) | BHJ, sol | 0.81 | 12.32 | 0.60 | 5.9 | [73] |
| ITO/ZnO (20 nm)/PBDTT-TT:**54** (3:7, 1 vol% DIO+1 vol% CN)/$MoO_x$ (5 nm)/Al (100 nm) | BHJ, sol | 0.80 | 13.7 | 0.56 | 6.1 | [74] |

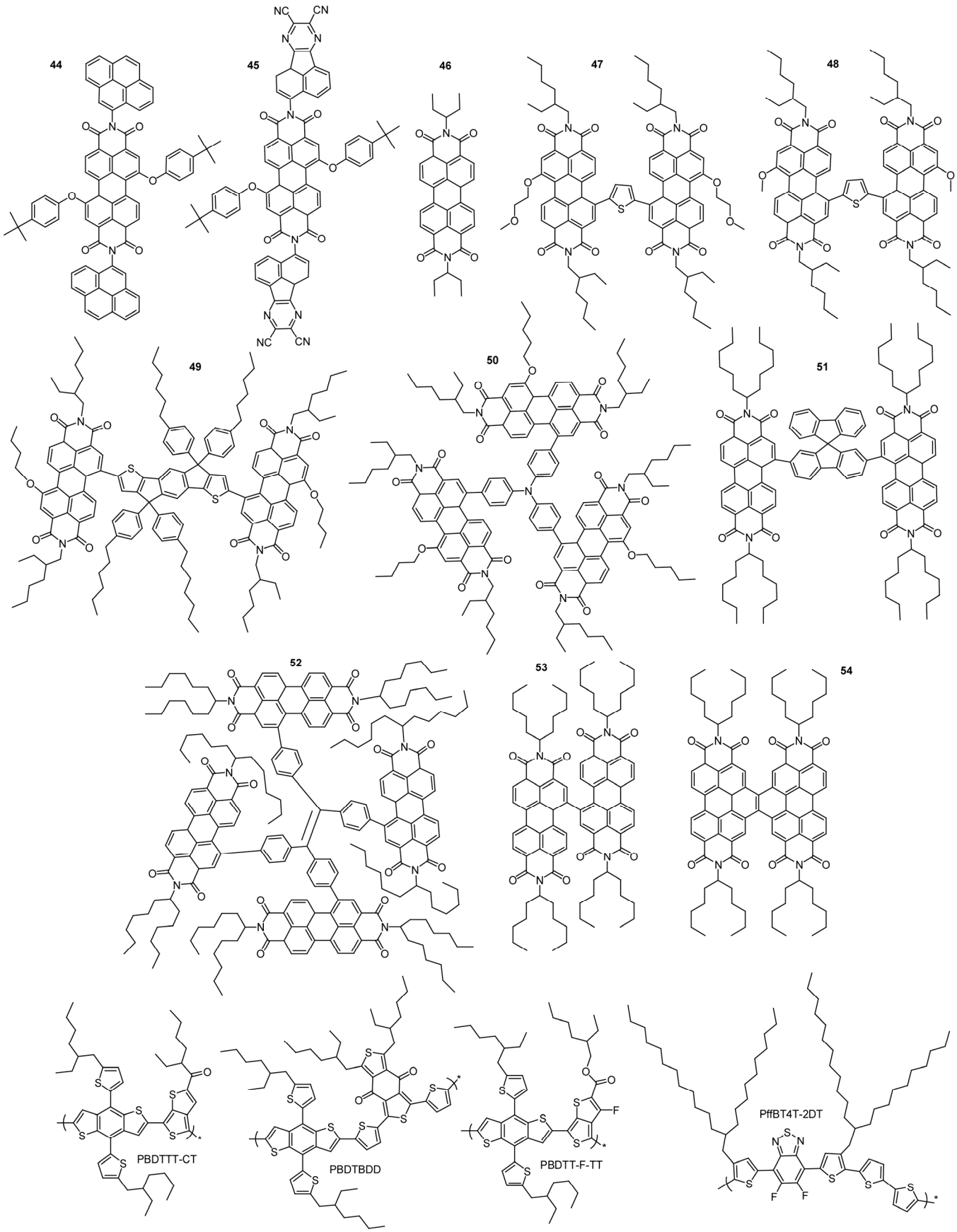


**Figure 8** PDI-based small molecule acceptors and polymer donors referred.

demonstrated that excitons generated in both donor and acceptor phases contribute to the photocurrent by effectively splitting at the donor-acceptor interfaces.

## 7 Conclusions

As shown above, representative small molecules exhibiting PCEs of over 5% for electron donors and over 3% for electron acceptors have been systematically reviewed. The intensive exploration towards high-performance small molecules being outlined here embodies abundant practical strategies and tricks, contributing to the achievements of high photovoltaic performance and further clarified the guidelines on molecular design to some extent. According to our observations, those strategies involved in current research can be divided into two aspects: (1) backbone engineering, which mainly includes the introduction or construction of new building blocks with variable electron-donating or -withdrawing properties or the substituent of the key atoms on the backbone with other heteroatoms, so as to adjust the energy level, bandgap, transport behavior, etc.; (2) accessory-group optimization, which comprises the adjustment of end groups, side chains, linkage units of the backbone. Such kind of tunings may not affect the optical and electrical properties too much, but generally play key roles in affecting the film reorganization after being processed in solution-processed devices, and thus induce the variation of final performance. The effect can be decisive under certain occasions. Besides, due to the lack of clear understanding on the effects of the kinetics of film formation, the molecule-orientated device optimization also comprise attractive topics for the researchers. For the development of non-fullerene acceptors, researches on PDIs would possibly still be dominative in future. Selecting appropriate linkage units to get finely controlled aggregation and transporting properties seems to be the major research direction. In addition, the appearance of several highly effective acceptors based on bulky fused-ring core also hints a probably emerging new series of non-fullerene acceptor materials [75]. Furthermore, particular attention should also be paid to other small molecules showing high PCEs yet not included within this review, such as SubPc and SubNc, showing an 8.4% PCE with a long-range exciton transfer when they were adopted as the co-acceptor [76], and heteropentacenes, a new series for vacuum deposited small molecules of 6.5% PCE, reported by Bäuerle *et al*. [77], both of which should be interesting cases capable of capturing scientific attention in this area.

*This work was supported by the National Basic Research Program of China (2014CB643502), the Strategic Priority Research Program of the Chinese Academy of Sciences (XDB12010200), and the National Natural Science Foundation of China (91333113).*

1 Choy WCH. *Organic Solar Cells*. London: Springer-Verlag, 2013
2 Shrotriya V. *Polymer Solar Cells: Achieving High Efficiency by Device Engineering and Morphology Control*. Saarbrücken: LAP Lambert Academic Publishing, 2010
3 a) Dou L, You J, Hong Z, Xu Z, Li G, Street RA, Yang Y. 25th Anniversary article: a decade of organic/polymeric photovoltaic research. *Adv Mater*, 2013, 25: 6642–6671; b) He F, Yu L. How far can polymer solar cells go? In need of a synergistic approach. *J Phys Chem Lett*, 2011, 2: 3102–3113; c) Brabec CJ, Gowrisanker S, Hall JJM, Laird D, Jia S, Williams SP. Polymer-fullerene bulk-heterojunction solar cells. *Adv Mater*, 2010, 22: 3839–3856; d) Boudreault PLT, Leclerc M. Processable low-bandgap polymers for photovoltaic applications. *Chem Mater*, 2011, 23: 456–469; e) Zhang ZG, Wang J. Structures and properties of conjugated donor-acceptor copolymers for solar cell applications. *J Mater Chem*, 2012, 22: 4178–4187; f) Thompson BC, Fréchet JMJ. Polymer-fullerene composite solar cells. *Angew Chem Int Ed*, 2007, 47: 58–77
4 a) Mishra A, Bauerle P. Small molecule organic semiconductors on the move: promises for future solar energy technology. *Angew Chem Int Ed*, 2012, 51: 2020–2067; b) Lin Y, Li Y, Zhan X. Small molecule semiconductors for high-efficiency organic photovoltaics. *Chem Soc Rev*, 2012, 41: 4245–4272; c) Chen YS, Wan XJ, Long GK. High performance photovoltaic applications using solution-processed small molecules. *Acc Chem Res*, 2013, 46: 2645–2655; d) Coughlin JE, Henson ZB, Welch GC, Bazan GC. Design and synthesis of molecular donors for solution-processed high-efficiency organic solar cells. *Acc Chem Res*, 2014, 47: 257–270
5 a) Liu Y, Zhao J, Li Z, Mu C, Ma W, Hu H, Jiang K, Lin Hao, Ade H, Yan H. Aggregation and morphology control enables multiple cases of high-efficiency polymer solar cells. *Nat Commun*, 2014, 5: 5293–5310; b) Liao S, Jhuo H, Yeh P, Cheng Y, Li Y, Lee Y, Sharma S, Chen S. Single junction inverted polymer solar cell reaching power conversion efficiency 10.31% by employing dual-doped zinc oxide nano-film as cathode interlayer. *Sci Rep*, 2014, 4: 6813–6819; c) Chen J, Cui C, Li Y, Zhou L, Ou Q, Li C, Li Y, Tang J. Single-junction polymer solar cells exceeding 10% power conversion efficiency. *Adv Mater*, 2015, 27: 1035–1041; d) Zhang S, Ye L, Zhao W, Yang B, Wang Q, Hou J. Realizing over 10% efficiency in polymer solar cell by device optimization. *Sci China Chem*, 2015, 58: 248–256
6 a) Kan B, Zhang Q, Li M, Wan X, Ni W, Long G, Wang Y, Yang X, Feng H, Chen Y. Solution-processed organic solar cells based on dialkylthiol-substituted benzodithiophene unit with efficiency near 10%. *J Am Chem Soc*, 2014, 136: 15529–15532; b) Zhang Q, Kan B, Liu F, Long G, Wan X, Chen X, Zuo Y, Ni W, Zhang H, Li M, Hu Z, Huang F, Cao Y, Liang Z, Zhang M, Russell PT, Chen Y. Small-molecule solar cells with efficiency over 9%. *Nat Photon*, 2015, 9: 35–41; c) Sun K, Xiao Z, Lu S, Zajaczkowski W, Pisula W, Hanssen E, White MJ, Williamson MR, Subbiah J, Ouyang J, Holmes BA, Wong W, Jones JD. A molecular nematic liquid crystalline material for high-performance organic photovoltaics. *Nat Commun*, 2015, 6: 6013–6021
7 Sun YM, Welch GC, Leong WL, Takacs CJ, Bazan GC, Heeger AJ. Solution-processed small-molecule solar cells with 6.7% efficiency. *Nat Mater*, 2012, 11: 44–48
8 Lin LY, Chen YH, Huang ZY, Lin HW, Chou SH, Lin F, Chen CW, Liu YH, Wong KT. A low-energy-gap organic dye for high-performance small-molecule organic solar cells. *J Am Chem Soc*, 2011, 133: 15822–15825
9 Chen YH, Lin LY, Lu CW, Lin F, Huang ZY, Lin HW, Wang PH, Liu YH, Wong KT, Wen JG, Miller DJ, Darling SB. Vacuum-deposited small-molecule organic solar cells with high power conversion efficiencies by judicious molecular design and device optimization. *J Am Chem Soc*, 2012, 134: 13616–13623
10 Lin HW, Lu CW, Lin LY, Chen YH, Lin WC, Wong KT, Lin F. Pyridine-based electron transporting materials for highly efficient

organic solar cells. *J Mater Chem A*, 2013, 1: 1770–1777
11 Lin HW, Chang JH, Huang WC, Lin YT, Lin LY, Lin F, Wong KT, Wang HF, Ho RM, Meng HF. Highly efficient organic solar cells using a solution processed active layer with a small molecule donor and pristine fullerene. *J Mater Chem A*, 2014, 2: 3709–3714
12 Lu HI, Lu CW, Lee YC, Lin HW, Lin LY, Lin F, Chang JH, Wu CI, Wong KT. New molecular donors with dithienopyrrole as the electron-donating group for efficient small-molecule organic solar cells. *Chem Mater*, 2014, 26: 4361–4367
13 Walker B, Kim C, Nguyen TQ. Small molecule solution-processed bulk heterojunction solar cells. *Chem Mater*, 2011, 23: 470–482
14 Loser S, Miyauchi H, Hennek JW, Smith J, Huang C, Facchetti A, Marks TJ. A "zig-zag" naphthodithiophene core for increased efficiency in solution-processed small molecule solar cells. *Chem Commun*, 2012, 48: 8511–8513
15 Li L, Huang Y, Peng J, Cao Y, Peng X. Enhanced performance of solution-processed solar cells based on porphyrin small molecules with a diketopyrrolopyrrole acceptor unit and a pyridine additive. *J Mater Chem A*, 2013, 1: 2144–2150
16 Huang JH, Zhan CL, Zhang X, Zhao Y, Lu ZH, Jia H, Jiang B, Ye J, Zhang SL, Tang AL, Liu YQ, Pei QB, Yao JN. Solution-processed DPP-based small molecule that gives high photovoltaic efficiency with judicious device optimization. *ACS Appl Mater Inter*, 2013, 5: 2033–2039
17 Lin YZ, Ma LC, Li YF, Liu YQ, Zhu DB, Zhan XW. A solution-processable small molecule based on benzodithiophene and diketopyrrolopyrrole for high-performance organic solar cells. *Adv Energy Mater*, 2013, 3: 1166–1170
18 Harschneck T, Zhou NJ, Manley EF, Lou SJ, Yu XG, Butler MR, Timalsina A, Turrisi R, Ratner MA, Chen LX, Chang RPH, Facchetti A, Marks TJ. Substantial photovoltaic response and morphology tuning in benzo[1,2-*b*:6,5-*b*′]-dithiophene (bBDT) molecular donors. *Chem Commun*, 2014, 50: 4099–4101
19 Qin H, Li L, Guo F, Su S, Peng J, Cao Y, Peng X. Solution-processed bulk heterojunction solar cells based on a porphyrin small molecule with 7% power conversion efficiency. *Energ Environ Sci*, 2014, 7: 1397–1401
20 Bura T, Leclerc N, Bechara R, Leveque P, Heiser T, Ziessel R. Triazatruxene-diketopyrrolopyrrole dumbbell-shaped molecules as photoactive electron donor for high-efficiency solution processed organic solar cells. *Adv Energy Mater*, 2013, 3: 1118–1124
21 Gao H, Li YQ, Wang LH, Ji CY, Wang Y, Tian WJ, Yang XC, Yin LX. High performance asymmetrical push-pull small molecules end-capped with cyanophenyl for solution-processed solar cells. *Chem Commun*, 2014, 50: 10251–10254
22 Silvestri F, Irwin MD, Beverina L, Facchetti A, Pagani GA, Marks TJ. Efficient squaraine-based solution processable bulk-heterojunction solar cells. *J Am Chem Soc*, 2008, 130: 17640–17641
23 Wei GD, Wang SY, Sun K, Thompson ME, Forrest SR. Solvent-annealed crystalline squaraine: PC70BM (1:6) solar cells. *Adv Energy Mater*, 2011, 1: 184–187
24 Wei GD, Xiao X, Wang SY, Zimmerman JD, Sun K, Diev VV, Thompson ME, Forrest SR. Arylamine-based squaraine donors for use in organic solar cells. *Nano Lett*, 2011, 11: 4261–4264
25 Wei GD, Xiao X, Wang SY, Sun K, Bergemann KJ, Thompson ME, Forrest SR. Functionalized squaraine donors for nanocrystalline organic photovoltaics. *ACS Nano*, 2012, 6: 972–978
26 Xiao X, Wei GD, Wang SY, Zimmerman JD, Renshaw CK, Thompson ME, Forrest SR. Small-molecule photovoltaics based on functionalized squaraine donor blends. *Adv Mater*, 2012, 24: 1956–1960
27 Zimmerman JD, Lassiter BE, Xiao X, Sun K, Dolocan A, Gearba R, Vanden Bout DA, Stevenson KJ, Wickramasinghe P, Thompson ME, Forrest SR. Control of interface order by inverse quasi-epitaxial growth of squaraine/fullerene thin film photovoltaics. *ACS Nano*, 2013, 7: 9268–9275
28 Lassiter BE, Zimmerman JD, Forrest SR. Tandem organic photovoltaics incorporating two solution-processed small molecule donor layers. *Appl Phys Lett*, 2013, 103: 123305
29 Fitzner R, Reinold E, Mishra A, Mena-Osteritz E, Ziehlke H, Korner C, Leo K, Riede M, Weil M, Tsaryova O, Weiss A, Uhrich C, Pfeiffer M, Bäuerle P. Dicyanovinyl-substituted oligothiophenes: structure-property relationships and application in vacuum-processed small-molecule organic solar cells. *Adv Funct Mater*, 2011, 21: 897–910
30 Fitzner R, Mena-Osteritz E, Mishra A, Schulz G, Reinold E, Weil M, Korner C, Ziehlke H, Elschner C, Leo K, Riede M, Pfeiffer M, Uhrich C, Bauerle P. Correlation of π-conjugated oligomer structure with film morphology and organic solar cell performance. *J Am Chem Soc*, 2012, 134: 11064–11067
31 Liu YS, Wan XJ, Wang F, Zhou JY, Long GK, Tian JG, You JB, Yang Y, Chen YS. Spin-coated small molecules for high performance solar cells. *Adv Energy Mater*, 2011, 1: 771–775
32 Li Z, He GR, Wan XJ, Liu YS, Zhou JY, Long GK, Zuo Y, Zhang MT, Chen YS. Solution processable rhodanine-based small molecule organic photovoltaic cells with a power conversion efficiency of 6.1%. *Adv Energy Mater*, 2012, 2: 74–77
33 Liu YS, Yang Y, Chen CC, Chen Q, Dou LT, Hong ZR, Li G, Yang Y. Solution-processed small molecules using different electron linkers for high-performance solar cells. *Adv Mater*, 2013, 25: 4657–4662
34 Liu YS, Wan XJ, Wang F, Zhou JY, Long GK, Tian JG, Chen YS. High-performance solar cells using a solution-processed small molecule containing benzodithiophene unit. *Adv Mater*, 2011, 23: 5387–5391
35 Zhou JY, Wan XJ, Liu YS, Long GK, Wang F, Li Z, Zuo Y, Li CX, Chen YS. A planar small molecule with dithienosilole core for high efficiency solution-processed organic photovoltaic cells. *Chem Mater*, 2011, 23: 4666–4668
36 Zhou JY, Wan XJ, Liu YS, Zuo Y, Li Z, He GR, Long GK, Ni W, Li CX, Su XC, Chen YS. Small molecules based on benzo[1,2-*b*:4,5-*b*′]dithiophene unit for high-performance solution-processed organic solar cells. *J Am Chem Soc*, 2012, 134: 16345–16351
37 Zhou JY, Zuo Y, Wan XJ, Long GK, Zhang Q, Ni W, Liu YS, Li Z, He GR, Li CX, Kan B, Li MM, Chen YS. Solution-processed and high-performance organic solar cells using small molecules with a benzodithiophene unit. *J Am Chem Soc*, 2013, 135: 8484–8487
38 Liu YS, Chen CC, Hong ZR, Gao J, Yang Y, Zhou HP, Dou LT, Li G, Yang Y. Solution-processed small-molecule solar cells: breaking the 10% power conversion efficiency. *Sci Rep*, 2013, 3: 3356–3363
39 Patra D, Huang TY, Chiang CC, Maturana ROV, Pao CW, Ho KC, Wei KH, Chu CW. 2-Alkyl-5-thienyl-substituted benzo[1,2-*b*:4,5-*b*′] dithiophene-based donor molecules for solution-processed organic solar cells. *ACS Appl Mater Inter*, 2013, 5: 9494–9500
40 Shen SL, Jiang P, He C, Zhang J, Shen P, Zhang Y, Yi YP, Zhang ZJ, Li ZB, Li YF. Solution-processable organic molecule photovoltaic materials with bithienyl-benzodithiophene central unit and indenedione end groups. *Chem Mater*, 2013, 25: 2274–2281
41 Deng D, Zhang Y, Yuan L, He C, Lu K, Wei Z. Effects of shortened alkyl chains on solution-processable small molecules with oxo-alkylated nitrile end-capped acceptors for high-performance organic solar cells. *Adv Energy Mater*, 2014, 4: 1400538
42 Wessendorf CD, Schulz GL, Mishra A, Kar P, Ata I, Weidelener M, Urdanpilleta M, Hanisch J, Mena-Osteritz E, Lindén M, Ahlswede E, Bäuerle P. Efficiency improvement of solution-processed dithieno-pyrrole-based A-D-A oligothiophene bulk-heterojunction solar cells by solvent vapor annealing. *Adv Energy Mater*, 2014, 4: 1400266
43 Bai HT, Wang YF, Cheng P, Li YF, Zhu DB, Zhan XW. Acceptor-donor-acceptor small molecules based on indacenodithiophene for efficient organic solar cells. *ACS Appl Mater Inter*, 2014, 6: 8426–8433
44 Leong WL, Welch GC, Kaake LG, Takacs CJ, Sun YM, Bazan GC,

Heeger AJ. Role of trace impurities in the photovoltaic performance of solution processed small-molecule bulk heterojunction solar cells. *Chem Sci*, 2012, 3: 2103–2109

45 Garcia A, Welch GC, Ratcliff EL, Ginley DS, Bazan GC, Olson DC. improvement of interfacial contacts for new small-molecule bulk-heterojunction organic photovoltaics. *Adv Mater*, 2012, 24: 5368–5373

46 van der Poll TS, Love JA, Nguyen TQ, Bazan GC. Non-basic high-performance molecules for solution-processed organic solar cells. *Adv Mater*, 2012, 24: 3646–3649

47 Love JA, Proctor CM, Liu JH, Takacs CJ, Sharenko A, van der Poll TS, Heeger AJ, Bazan GC, Nguyen TQ. Film morphology of high efficiency solution-processed small-molecule solar cells. *Adv Funct Mater*, 2013, 23: 5019–5026

48 Kyaw AKK, Wang DH, Gupta V, Leong WL, Ke L, Bazan GC, Heeger AJ. Intensity dependence of current-voltage characteristics and recombination in high-efficiency solution-processed small-molecule solar cells. *ACS Nano*, 2013, 7: 4569–4577

49 Wang DH, Kyaw AKK, Gupta V, Bazan GC, Heeger AJ. Enhanced efficiency parameters of solution-processable small-molecule solar cells depending on ITO sheet resistance. *Adv Energy Mater*, 2013, 3: 1161–1165

50 Gupta V, Kyaw AKK, Wang DH, Chand S, Bazan GC, Heeger AJ. Barium: an efficient cathode layer for bulk-heterojunction solar cells. *Sci Rep*, 2013, 3: 1965–1970

51 Xu XY, Kyaw AKK, Peng B, Du QG, Hong L, Demir HV, Wong TKS, Xiong QH, Sun XW. Enhanced efficiency of solution-processed small molecule solar cells upon incorporation of gold nanospheres and nanorods into organic layers. *Chem Commun*, 2014, 50: 4451–4454

52 Liu XF, Sun YM, Hsu BBY, Lorbach A, Qi L, Heeger AJ, Bazan GC. Design and properties of intermediate-sized narrow band-gap conjugated molecules relevant to solution-processed organic solar cells. *J Am Chem Soc*, 2014, 136: 5697–5708

53 Love JA, Nagao I, Huang Y, Kuik M, Gupta V, Takacs CJ, Coughlin JE, Qi L, van der Poll TS, Kramer EJ, Heeger AJ, Nguyen TQ, Bazan GC. Silaindacenodithiophene-based molecular donor: morphological features and use in the fabrication of compositionally tolerant high-efficiency bulk heterojunction solar cells. *J Am Chem Soc*, 2014, 136: 3597–3606

54 Sun Y, Seifter J, Huo L, Yang Y, Hsu BBY, Zhou H, Sun X, Xiao S, Jiang L, Heeger AJ. High-performance solution-processed small-molecule solar cells based on a dithienogermole-containing molecular donor. *Adv Energy Mater*, 2015, 5: 1400987

55 Lim K, Lee SY, Song K, Sharma GD, Ko J. Synthesis and properties of low bandgap star molecules TPA-[DTS-PyBTTh$_3$]$_3$ and DMM-TPA [DTS-PyBTTh$_3$]$_3$ for solution-processed bulk hetero-junction organic solar cells. *J Mater Chem C*, 2014, 2: 8412–8422

56 a) Sonar P, Lim JPF, Chan KL. Organic non-fullerene acceptors for organic photovoltaics. *Energy Environ Sci*, 2011, 4: 1558–1574; b) Lin Y, Zhan X. Non-fullerene acceptors for organic photovoltaics: an emerging horizon. *Mater Horiz,*. 2014, 1: 470–488; c) Eftaiha AF, Sun JP, Hill IG, Welch GC. Recent advances of non-fullerene small molecular acceptors for solution processed bulk heterojunction solar cells. *J Mater Chem A*, 2014, 2: 1201–1213; d) Anthony JE. Small-molecule nonfullerene acceptors for polymer bulk heterojunction organic photovoltaics. *Chem Mater*, 2011, 23: 583–590

57 a) Sullivan P, Duraud A, Hancox I, Beaumont N, Mirri G, Tucker HRJ, Hatton AR, Shipman M, Jones ST. Halogenated boron subphthalocyanines as light harvesting electron acceptors in organic photovoltaics. *Adv Energy Mater*, 2011, 1: 352–355; b) Bloking JT, Han X, Higgs AT, Kastrop JP, Pandey L, Norton JE, Risko C, Chen CE, Bredas JL, McGehee MD, Sellinger A. Solution-processed organic solar cells with power conversion efficiencies of 2.5% using benzothiadiazole/imide-based acceptors. *Chem Mater*, 2011, 23: 5484–5490; c) Verreet B, Rand BP, Cheyns D, Hadipour A, Aernouts T, Heremans P, Medina A, Claessens CG, Torres T. A 4% efficient organic solar cell using a fluorinated fused subphthalocyanine dimer as an electron acceptor. *Adv Energy Mater*, 2011, 1: 565–568; d) Zheng YQ, Dai YZ, Zhou Y, Wang JY, Pei J. Rational molecular engineering towards efficient non-fullerene small molecule acceptors for inverted bulk heterojunction organic solar cells. *Chem Commun*, 2014, 50: 1591–1594

58 Sharma GD, Suresh P, Mikroyannidis JA, Stylianakis MM. Efficient bulk heterojunction devices based on phenylenevinylene small molecule and perylene-pyrene bisimide. *J Mater Chem*, 2010, 20: 561–567

59 Mikroyannidis JA, Suresh P, Sharma GD. Synthesis of a perylene bisimide with acetonaphthopyrazine dicarbonitrile terminal moieties for photovoltaic applications. *Synth Met*, 2010, 160: 932–938

60 Sharenko A, Proctor CM, van der Poll TS, Henson ZB, Nguyen TQ, Bazan GC. A high-performing solution-processed small molecule: perylene diimide bulk heterojunction solar cell. *Adv Mater*, 2013, 25: 4403–4406

61 Singh R, Aluicio-Sarduy E, Kan Z, Ye T, MacKenzie RCI, Keivanidis PE. Fullerene-free organic solar cells with an efficiency of 3.7% based on a low-cost geometrically planar perylene diimide monomer. *J Mater Chem A*, 2014, 2: 14348–14353

62 Rajaram S, Shivanna R, Kandappa KS, Narayan SK. Nonplanar perylene diimides as potential alternatives to fullerenes in organic solar cells. *J Phys Chem Lett*, 2012, 3: 2405–2408

63 Zhang X, Lu ZH, Ye L, Zhan CL, Hou JH, Zhang SQ, Jiang B, Zhao Y, Huang JH, Zhang SL, Liu Y, Shi Q, Liu YQ, Yao JN. A potential perylene diimide dimer-based acceptor material for highly efficient solution-processed non-fullerene organic solar cells with 4.03% efficiency. *Adv Mater*, 2013, 25: 5791–5797

64 Lu ZH, Jiang B, Zhang X, Tang AL, Chen LL, Zhan CL, Yao JN. Perylene-diimide based non-fullerene solar cells with 4.34% efficiency through engineering surface donor/acceptor compositions. *Chem Mater*, 2014, 26: 2907–2914

65 Zhang X, Zhan C, Yao J. Non-fullerene organic solar cells with 6.1% efficiency through fine-tuning parameters of the film-forming process. *Chem Mater*, 2015, 27: 166–173

66 Lin YZ, Wang JY, Dai SX, Li YF, Zhu DB, Zhan XW. A twisted dimeric perylene diimide electron acceptor for efficient organic solar cells. *Adv Energy Mater*, 2014, 4: 1400420

67 Lin YZ, Wang YF, Wang JY, Hou JH, Li YF, Zhu DB, Zhan XW. A star-shaped perylene diimide electron acceptor for high-performance organic solar cells. *Adv Mater*, 2014, 26: 5137–5142

68 Zhao J, Li Y, Lin H, Liu Y, Jiang K, Mu C, Ma T, Lai J, Hu H, Yan H. High-efficiency non-fullerene organic solar cells enabled by a difluorobenzothiadiazole-based donor polymer combined with a properly matched small molecule acceptor. *Energy Environ Sci*, 2015, 8: 520–525

69 Yan Q, Zhou Y, Zheng Y, Pei J, Zhao D. Towards rational design of organic electron acceptors for photovoltaics: a study based on perylenediimide derivatives. *Chem Sci*, 2013, 4: 4389–4394

70 Liu Y, Mu C, Jiang K, Zhao J, Li Y, Zhang L, Li Z, Lai J, Hu H, Ma T, Hu R, Yu D, Huang X, Tang B, Yan H. A tetraphenylethylene core-based 3D structure small molecular acceptor enabling efficient non-fullerene organic solar cells. *Adv Mater*, 2015, 27: 1015–1020

71 Jiang W, Ye L, Li X. G, Xiao CY, Tan F, Zhao WC, Hou JH, Wang ZH. Bay-linked perylene bisimides as promising non-fullerene acceptors for organic solar cells. *Chem Commun*, 2014, 50: 1024–1026

72 Ye L, Jiang W, Zhao W, Zhang S, Qian D, Wang Z, Hou J. Selecting a donor polymer for realizing favorable morphology in efficient non-fullerene acceptor-based solar cells. *Small*, 2014, 10: 4658–4663

73 Zang Y, Li CZ, Chueh CC, Williams ST, Jiang W, Wang ZH, Yu JS, Jen AKY. Integrated molecular interfacial, and device engineering towards high-performance non-fullerene based organic solar cells. *Adv Mater*, 2014, 26: 5708–5714

74 Zhong Y, Trinh MT, Chen R, Wang W, Khlyabich PP, Kumar B, Xu Q, Nam CY, Sfeir MY, Black C, Steigerwald ML, Loo YL, Xiao S, Ng F, Zhu XY, Nuckolls C. Efficient organic solar cells with helical perylene diimide electron acceptors. *J Am Chem Soc*, 2014, 136: 15215–15221

75 a) Lin Y, Zhang Z, Bai H, Wang J, Yao Y, Li Y, Zhu D, Zhan X. High-performance fullerene-free polymer solar cells with 6.31% efficiency. *Energy Environ Sci*, 2015, 8: 610–616; b) Lin Y, Wang J, Zhang Z, Bai H, Li Y, Zhu D, Zhan X. An electron acceptor challenging fullerenes for efficient polymer solar cells. *Adv Mater*, 2015, 27: 1170–1174

76 Cnops K, Rand BP, Cheyns D, Verreet B, Empl MA, Heremans P. 8.4% Efficient fullerene-free organic solar cells exploiting long-range exciton energy transfer. *Nat Commun*, 2014, 5: 3406–3411

77 Mishra A, Popovic D, Vogt A, Kast H, Leitner T, Walzer K, Pfeiffer M, Mena-Osteritz E, Bäuerle P. A-D-A-type *S*,*N*-heteropentacenes: next-generation molecular donor materials for efficient vacuum-processed organic solar cells. *Adv Mater*, 2014, 26: 7217–7223